JOURNAL OF VIROLOGY, Jan. 1994, p. 93–102
0022-538X/94/$04.00+0

Vol. 68, No. 1

Temporal Patterns of Human Immunodeficiency Virus Type 1 Transcripts in Human Fetal Astrocytes

CARLO TORNATORE,* KAREN MEYERS, WALTER ATWOOD, KATHERINE CONANT, AND EUGENE MAJOR

Laboratory of Molecular Medicine and Neuroscience, National Institute of Neurological Disorders and Stroke, Bethesda, Maryland 20892

Received 3 August 1993/Accepted 5 October 1993

Human immunodeficiency virus type 1 (HIV-1) infection of the developing central nervous system results in a dementing process in children, termed HIV-1-associated encephalopathy. Infection of astroglial elements of the pediatric nervous system has been demonstrated and suggests that direct infection of some astrocytes may contribute to the neurologic deficit. In this model, HIV-1 establishes a persistent state of infection in astrocytes, which can be reactivated by the cytokines tumor necrosis factor alpha (TNF-α) and interleukin 1β (IL-1β). To better understand the natural history of viral persistence in astroglial cells, we characterized infection at the transcriptional level. The most abundant viral transcript during the establishment of persistence was the subgenomic multiply spliced 2-kb message, similar to mononuclear cell models of HIV-1 latency. Following reactivation with TNF-α or IL-1β the multiply spliced 2-kb message remained the most abundant viral transcript, in contrast to infected mononuclear cells in which reactivation leads to the reemergence of the 9- and 4-kb transcripts. Further characterization of the persistent 2-kb transcript by PCR amplification of in vitro-synthesized viral cDNA showed that, in the absence of cytokine stimulation, the most abundant multiply spliced transcripts were the Nef- and Rev-specific messages. However, following cytokine stimulation, double- and triple-spliced Tat-, Rev-, and Nef-specific messages could be identified. Immunohistochemical staining demonstrated that, during viral persistence, astrocytes expressed Nef protein but few or no viral structural proteins. These results demonstrate that viral persistence in astrocytes at the transcriptional level is fundamentally different from that seen in mononuclear cells and could account for the virtual absence of astroglial expression of viral structural antigens in vivo.

Vertically transmitted human immunodeficiency virus type 1 (HIV-1) infection is now among the top five leading causes of death in children <4 years of age (34). Of those children infected with HIV-1, approximately one-third to two-thirds will go on to develop manifestations of central nervous system (CNS) dysfunction characterized by a loss of developmental milestones involving both motor and cognitive systems (4, 18). This constellation of neurologic signs and symptoms has been termed pediatric AIDS encephalopathy, which has as its parallel the dementia seen in adults infected with HIV-1 (32, 36). The pathogenesis of AIDS-related encephalopathy remains elusive. The neuropathological hallmarks of HIV-1 infection of the CNS have been well described, consisting of infiltrating macrophages, multinucleated giant cells, and reactive microglial cells associated with widespread astrogliosis, myelin pallor, and neuronal loss (31, 36, 44). While cells of the mononuclear lineage have consistently been demonstrated to express viral antigens and to harbor viral nucleic acids in the nervous system, the number of infected cells is small relative to the widespread neuropathology. To explain this discrepancy, it has been proposed that the effects of mononuclear infection indirectly lead to the parenchymal changes. This is supported by data which demonstrate that infected monocytes can elaborate HIV-1 gene products and other cellular factors which are neurotoxic (5, 9, 15, 20, 21, 25, 37).

Direct infection of the neuronal and astroglial elements of the CNS has also been proposed to contribute to HIV-1-associated dementia. An early description of pediatric HIV-1-associated neuropathology demonstrated the presence of viral particles in astrocytes (17), suggesting that the immature elements in the developing nervous system were susceptible to HIV-1 infection during vertical transmission. In vitro infection of human fetal astrocytes, as well as astrocytoma cell lines, has subsequently been demonstrated (8, 10–12, 14, 49). HIV-1 establishes a persistent state of infection in astroglial cells, which can be reactivated by the cytokines tumor necrosis factor alpha (TNF-α) and interleukin 1β (IL-1β) (49), an activation mediated by the induction of NF-κB (47).

To better understand the mechanisms which may underlie the establishment of persistent infection of astrocytes, we examined the temporal appearance of HIV-1 mRNA in human fetal astrocytes. We report that during the establishment of persistence, at times of little or no p24 or gp41 expression, the predominant viral transcript seen by Northern (RNA) hybridization was the subgenomic, multiply spliced 2-kb message. Reactivation with TNF-α or IL-1β resulted in a brief phase of viral replication with expression of p24 and gp41; however, the multiply spliced message remained the most abundant viral transcript. Using reverse transcriptase (RT)-PCR technology to identify the subpopulations represented in the 2-kb transcripts, we found that during periods of viral persistence the most abundant regulatory transcripts were those which coded for Nef and Rev (Nef- and Rev-specific transcripts) with a predominance of the Nef-specific transcripts. In contrast, following stimulation with TNF-α or IL-1β, doubly and triply spliced Tat-, Rev-, and Nef-specific messages could be identified within 24 h. Immunohistochemical staining of astrocytes persistently infected with HIV-1 further revealed expression of Nef protein in these cells at times when little viral structural protein could be detected.

* Corresponding author.

MATERIALS AND METHODS

Cell cultures from brain tissue. Cultures from human fetal brain tissue were prepared as described previously (49). Brain tissue was dissected from 9- to 14-week-old human fetuses, mechanically disrupted by aspiration through a 19-gauge needle, washed in Eagle's minimum essential medium (E-MEM) and plated into poly-D-lysine (0.1 mg/ml in distilled water)-treated tissue culture flasks. Each brain specimen was plated separately without pooling of tissues from fetuses of similar or different gestational ages. Cultures were maintained and fed every 3 to 4 days with E-MEM plus 10% fetal bovine serum. To prepare pure cultures of astrocyte cells, the cultures were first refed with serum-free medium and placed in an orbital shaker (210 rpm) at 37°C for 2 h. Cells released from the cultures were discarded while the adherent cells were refed with medium with serum. For serial passage, cells were harvested with 0.025% trypsin and 0.005% EDTA, counted in an hemocytometer, and plated at 10^6 in 100-mm-diameter plates. Following two to four passages, the cultures were stained with an antibody to glial acidic fibrillary protein (DAKO) to determine the percentage of cells which were astrocytes. Only those cultures which were 99% glial acidic fibrillary protein antibody positive were used.

Transfection procedure. The calcium phosphate precipitation technique was used for transfection. Five micrograms of uncleaved plasmid DNA per plate was used. The DNA was precipitated in HEPES (*N*-2-hydroxyethylpiperazine-*N'*-2-ethanesulfonic acid [pH 7.1]) buffer (137 mM NaCl, 5 mM KCl, 0.7 mM Na_2HPO_4, 6 mM dextrose, 21 mM HEPES) with 125 mM $CaCl_2$ for the final concentration. The DNA in HEPES buffer was kept at room temperature for 30 min for precipitate formation. The cell cultures were washed in HEPES buffer prior to addition of the DNA precipitate. The HEPES-DNA precipitate was placed directly on the cells for 30 min at room temperature, and then the cells were refed with E-MEM. Following a 4-h incubation at 37°C, the cells were washed three times with E-MEM, shocked with 15% glycerol in E-MEM for 45 s, and then washed three more times with E-MEM.

Immunodetection assays. Cells were plated on glass coverslips, fixed in acetone and methanol for 10 min each at −20°C, and washed in phosphate-buffered saline (PBS [pH 7.1]). All remaining incubations were performed at room temperature. Endogenous peroxidase activity was quenched for 30 min in 3% hydrogen peroxide in methanol. The cells were then blocked with 3% normal goat serum for 20 min, followed by incubation with a primary antibody (either a mouse monoclonal antibody to Nef protein diluted 1:250 [AIDS Research and Reference Reagent Program, catalog no. 1123], a rabbit polyclonal antibody to glial acidic fibrillary protein [DAKO], or a mouse monoclonal antibody to HIV-1 gp41 [Genetic Systems]). The incubation time for the glial acidic fibrillary protein and gp41 antibodies was 1 h, while the Nef antibody was incubated for 24 h. Cells were then washed in PBS and incubated with either biotinylated anti-rabbit or anti-mouse immunoglobulin G for 1 h. Following a wash in PBS, the cells were incubated with peroxidase-conjugated streptavidin for 60 min. Color was then developed with a fresh solution of diaminobenzidine tetrahydrochloride, resulting in a brown precipitate. Slides were then washed, counterstained with hematoxylin, dehydrated in graded alcohols, and mounted with Permount (Fisher Scientific).

Cytokines. All cytokines used were either human recombinants or were derived from a human cell source (Boehringer Mannheim). Cytokines were stored in aliquots at −20°C following reconstitution in E-MEM with 10% fetal calf serum. Aliquots were thawed only once. The concentrations of cytokines used were as follows: TNF-α, 10 ng/ml; IL-1β, 10 U/ml.

Cytoplasmic RNA extraction. Following transfection, cytoplasmic RNA was isolated from cells in 100-mm-diameter tissue culture dishes (1×10^6 to 5×10^6 cells). Prior to this procedure, all of the reagents were treated with 0.1% diethylpyrocarbonate to inhibit RNases. The cells were placed at 4°C for 30 to 60 min, washed and harvested by mechanical scraping in cold 1× PBS, and pelleted by centrifugation at 14,000 rpm for 30 s at 4°C. The cells were resuspended in 270 μl of cold Iso-High (0.14 M NaCl, 10 mM Tris [pH 8.4], 1.5 mM $MgCl_2$) and 30 μl of cold 5% Nonidet P-40 in H_2O. After incubation on ice for 2 min, the nuclei were pelleted by centrifugation at 14,000 rpm for 30 s at 4°C in an Eppendorf microcentrifuge. The supernatant was extracted twice in phenol-chloroform (1:1 ratio) and once in chloroform alone, followed by precipitation of the RNA in 70% ethanol at −20°C. RNA was collected by centrifugation at 14,000 rpm, resuspended in TES buffer (10 mM Tris [pH 7.5], 1 mM EDTA, 0.05% sodium dodecyl sulfate [SDS]) and reprecipitated in 1/10 volume of 3 M sodium acetate (pH 5.5) and 70% ethanol at −20°C for several hours. Following centrifugation at 14,000 rpm, the RNA pellet was air dried and resuspended in water.

Total RNA extraction. Total RNA was also extracted from parallel cultures of transfected astrocyte cultures by a previously described protocol (54).

Northern hybridization. RNA extraction samples were analyzed by electrophoresis in 1× MOPS buffer {0.02 M MOPS (3-[*N*-morpholino]propanesulfonic acid), 0.005 M NaHAc, 0.001 M EDTA} on 1.0% horizontal agarose gels containing 0.62 M formaldehyde. Following electrophoresis, the gel was rinsed once for 20 min with 0.05 N NaOH, followed by a 20-min wash in 20× SSPE (3.0 M NaCl, 0.2 M NaH_2PO_4, 0.02 M EDTA-Na_2). The remaining steps of the Northern transfer and hybridization are identical to those of the Southern transfer and hybridization described below. The probe used for Northern hybridization was an 8,088-bp fragment of pNL4-3 (1) generated by endonuclease *Ava*I digestion and nick translation with a ^{32}P-labeled dATP.

cDNA synthesis and PCR amplification. One microgram of either total or cytoplasmic RNA was heated at 65°C for 5 min and cooled on ice. First-strand synthesis of cDNA was carried out in a total volume of 20 μl consisting of 50 mM KCL, 10 mM Tris-HCl, 5 mM $MgCl_2$, 1 mM each deoxynucleoside triphosphate (dNTP), 20 U of RNase inhibitor (Perkin-Elmer), 50 U of Moloney murine leukemia virus RT (Perkin-Elmer), 1 μg of template RNA, and 1 μg of an antisense oligonucleotide primer. For reverse transcription of the multiply spliced mRNAs, the oligonucleotide *Bam*A located in exon 7 at the *Bam*HI site was used. The sequence and location of *Bam*A in pNL4-3 are 5′-GCTAAGGATCCGTTCACTAATCGAAT GG-3′ and nucleotides (nt) 8472 to 8448, respectively. For reverse transcription of the *gag* region of the 9-kb viral transcript, the oligonucleotide SK431 was used. The sequence and location of SK431 in pNL4-3 are 5′-TGCTATGTCACT TCCCCTTGGTTCTCT-3′ and nt 1500 to 1474, respectively. The reaction mixture was incubated at 45°C for 1 h, followed by incubation at 95°C for 5 min. PCR amplification of the single-stranded DNA was carried out by bringing the cDNA reaction mixture up to a final volume of 100 μl consisting of 50 mM KCL, 10 mM Tris-HCl, 2 mM $MgCl_2$, 0.2 mM each dNTP, 2.5 U of Ampli-*taq* DNA polymerase (Perkin-Elmer), and 1 μg of a sense primer. For amplification of the multiply spliced transcripts, the oligonucleotide *Bss*, located in exon 1 at the

*Bss*HII site, was added. The sequence and location of *Bss* in pNL4-3 are 5'-GGCTTGCTGAAGCGCGCACGGCAAG AGG-3' and nt 700 to 727, respectively. For amplification of the *gag* region of the 9-kb transcript, the oligonucleotide SK145 was used. The sequence and location of SK145 are 5'-AGTGGGGGGACATCAAGCAGCCATGCAAAT-3' and nt 1359 to 1388, respectively. The reaction mixture was denatured at 94°C for 1 min, primers were annealed at 55°C for 2 min, and primers were extended at 72°C for 3 min for a total of 40 cycles in a DNA thermal cycler (Perkin-Elmer Cetus). Ten microliters of each PCR product was run on a 1.5% agarose horizontal gel, stained with ethidium bromide, visualized with UV light, and photographed.

Southern transfer and hybridization. To further ensure the specificity of the PCR products, all reaction mixtures underwent Southern blot transfer. The agarose gel was rinsed once with distilled water and then denatured twice in 1 M NaCl–0.5 M NaOH for 15 min. This was followed by neutralization in 0.5 M Tris–1.5 M NaCl for 15 min, which was also done twice. The DNA was transferred to a nylon filter by capillary action, cross-linked by UV radiation (Stratalinker; Stratagene), and prehybridized in 50% formamide–6× SSPE (0.9 M NaCl, 0.06 M NaH_2PO_4, 0.006 M EDTA-Na_2)–5× Denhardt's solution–0.5% SDS–100 μg of calf thymus DNA per ml at 42°C for 1 h. The filter was hybridized in an identical solution which also contained 10^6 dpm of a ^{32}P-labeled nick-translated 8,088-bp *Ava*I fragment of pNL4-3 per ml (1). The probe was allowed to hybridize to the filter at 42°C for at least 16 h. The filter was washed twice in 6× SSPE–0.1% SDS for 30 min at room temperature. This was followed by two washes in 1× SSPE–0.5% SDS for 30 min at 64°C and a final wash in 0.1× SSPE–0.5% SDS for 30 min at 64°C. The filter was dried and used for autoradiography.

Following autoradiography, the filter was stripped of the radiolabeled probe in 50% formamide–2× SSPE at 65°C for 90 min. The filter was then sequentially hybridized with the following series of oligonucleotide probes (labeled with [γ-^{32}P]ATP with T4 polynucleotide kinase [New England Biolabs]): oligonucleotide 2, located in exon 2 at nt 4962 to 4945, 5'-CTTTCCAGAGGAGCTTTG; oligonucleotide 3, located in exon 3 at nt 5446 to 5429, 5'GATATTCACACCTAG GAC; oligonucleotide 4 *tat*, located in the 5' portion of exon 4 at nt 5803 to 5780, 5'-CCTATTCTGCTATGTCGACACCCA-3'; oligonucleotide 4a/b *tat/rev*, located in exon 4a/b at nt 5981 to 5959, 5'-TTCCTGCCATAGAGATGCC-3'; and oligonucleotide 5 *tat/rev/nef*, located in the 5' portion of exon 5 at nt 5997 to 5979, 5'-TCGCTGTCTCCGCTTCTTC-3'.

To detect the PCR products generated by primers SK145 and SK431, the internal oligonucleotide SK102 was used. SK102 is located in the *gag* gene at nt 1396 to 1428 and has the sequence 5'-GAGACCATCAATGAGGAAGCTGCAGAAT GGGAT-3'.

RESULTS

Temporal characteristics of p24 production in pNL4-3-transfected astrocyte cultures. We have previously described the kinetics of p24 production in human fetal astrocytes following transfection with the infectious molecular clone pNL4-3 (1, 49). The brief productive phase of viral replication seen immediately posttransfection is followed by a persistent phase during which little p24 is produced. As seen in Fig. 1, the application of the cytokine TNF-α results in brief bursts of p24 production (similar results were found for IL-1). Furthermore, in the current set of experiments, we found that the longer the cells remain in a state of viral persistence, the more attenuated

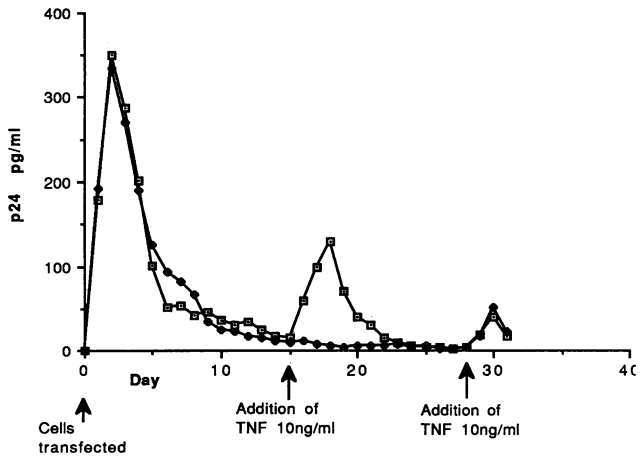

FIG. 1. Temporal characteristics of p24 production in pNL4-3-transfected astrocyte cultures stimulated at different time points with TNF-α. Two separate cultures of human astrocytes were established and transfected in parallel. The concentration of p24 protein in the supernatant fluid was determined every 24 h by using an antigen-capture enzyme-linked immunosorbent assay (ELISA [Coulter]). At each time point, the culture medium was collected and replaced with fresh medium. Each datum point represents the mean value of three experiments. Cytokines were added to the medium only on the day noted on the graph. At day 15, TNF was only added to one set of cultures (⊡). At day 27, TNF was added to both sets.

the effects of cytokine administration were. As seen in Fig. 1, if TNF-α is added to the cultures 2 weeks posttransfection, the p24 levels rise to approximately 100 to 150 pg/ml from a baseline of approximately 15 pg/ml. However, if TNF-α is added to the cultures 4 weeks posttransfection, the p24 levels rise to a p24 level of approximately 50 pg/ml from a baseline of <1 pg/ml. This phenomenon is independent of prior cytokine stimulation and appears to be a function of time from initial transfection.

As noted previously (49) and in a subsequent section of this paper (see section on temporal characteristics of Tat-, Rev-, and Nef-specific transcripts in astrocytes), supernatant from cytokine-treated cultures was infectious, as demonstrated by incubation of the supernatant with the CD4$^+$ lymphoblastoid cell line A3.01 (19).

Temporal characteristics of HIV-1 mRNA transcripts in astrocytes. To better understand the mechanisms which underlie the establishment of viral persistence in astrocytes, we next characterized the temporal characteristics of viral mRNA production during the establishment of persistence and in response to cytokine stimulation. As seen in Fig. 2, 2 days posttransfection all three viral transcripts could be identified as unspliced (9 kb), singly spliced (4 kb), and multiply spliced (2 kb), with the multiply spliced message being the most abundant. By day 15, when p24 levels were approaching the baseline, only the multiply spliced transcript was evident. The addition of either IL-1 or TNF-α on day 15 led to a marked increase in the multiply spliced transcripts within 24 h. While there was not a detectable increase in the unspliced or singly spliced transcripts, there was a rise in the levels of p24 in the culture supernatant (as seen in Fig. 1), suggesting that the number of singly spliced or unspliced transcripts was below the sensitivity levels of Northern blotting. Northern blots done 48 and 72 h after cytokine administration, at times of peak p24 production, were no different from the blot seen in Fig. 2.

By day 27 posttransfection, viral transcripts could not be

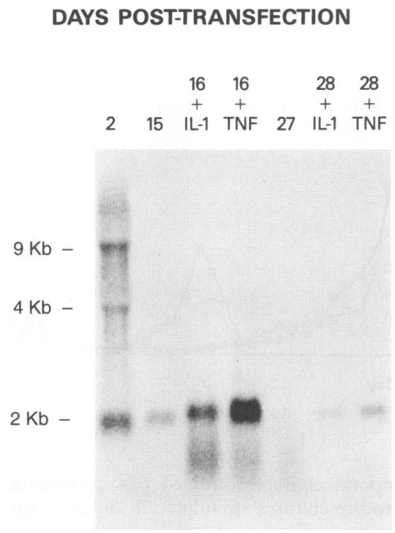

FIG. 2. Temporal characteristics of HIV-1 mRNA transcripts in astrocytes. RNA was purified at different time points from astrocytes transfected with pNL4-3. RNA was extracted from cytokine-stimulated astrocytes 24 h after the addition of either TNF-α or IL-1β on day 15 or 27 posttransfection. Northern transfer and hybridization were done as described in the text. The approximate sizes of the transcripts are given on the left.

TABLE 1. Comparison of *gag* gene transcription and expression in astrocytes at different time points posttransfection

Days post-transfection	p24 levels (pg/ml) in cell supernatant	Intracellular p24 levels (pg/10^6 cells)[a]	Presence of *gag* portion of 9-kb transcript as detected by RT-PCR[b]	Presence of 9-kb transcript as detected by Northern hybridization[b]
2	358	108	+	+
15	42	<1	+	−
16 + TNF[c]	146	28	+	−
27	<1	<1	−	−
28 + TNF	48	11	+	−

[a] Intracellular p24 levels were determined as follows. Cells (10^6) were washed, resuspended in 1 ml of serum-free medium, and vortexed for 5 min. The cellular debris was pelleted, and the supernatant was removed. The supernatant was mixed with 0.5 ml of 70% sorbitol and 0.5 ml of 100% fetal calf serum and assayed for p24 antigen with an antigen-capture ELISA (Coulter).

[b] +, present; −, not present.

[c] + TNF denotes administration of cytokines 24 h prior to the ELISA.

detected in astrocyte cultures which had had no prior cytokine stimulation. Addition of either TNF-α or IL-1β on day 27 posttransfection to astrocytes in a state of viral persistence again led to the induction of the multiply spliced 2-kb message within 24 h, although it was a significantly weaker signal than that induced at day 16 posttransfection.

Northern hybridization blots with total RNA from transfected cells were no different from hybridization with cytoplasmic RNA.

Given the absence of the 9- and 4-kb transcripts at times of cytokine stimulation, a series of studies were done to determine whether the cytokine-induced rise in p24 levels in the cell supernatant resulted from de novo synthesis of p24 from nascent viral transcripts versus release of previously synthesized p24 in the absence of viral transcripts. In the first set of experiments, five parallel astrocyte cultures were established and transfected and the p24 levels in the cell supernatant and intracellularly were measured at different time points. As summarized in Table 1, the presence or absence of p24 in the supernatant was paralleled by the presence of absence of p24 intracellularly. At day 27, no intracellular or extracellular p24 was detectable. However, 24 h following cytokine stimulation, p24 was again detectable in both the supernatant and intracellularly, demonstrating that cytokine-induced rises in p24 resulted from de novo synthesis of the core protein. The second set of experiments attempted to identify the 9-kb viral transcript by a more sensitive method than Northern hybridization. For this, we utilized an RT-PCR method in which RNA used in the Northern hybridization was reverse transcribed with the primer SK431 and then was PCR amplified with primers SK145 and SK431. The primer set SK145 and SK431 amplified a 142-bp fragment of the *gag* region of the 9-kb transcript, a region which is spliced out of the 4- and 2-kb viral transcripts. Following gel electrophoresis and Southern transfer, the PCR products were hybridized with an end-labeled internal probe, SK102. As summarized in Table 1, RT-PCR was able to detect the 9-kb transcript at times when Northern hybridization could not. Furthermore, the presence or absence of the 9-kb transcript as detected by RT-PCR paralleled the presence or absence of p24 in the culture system. In total, these experiments suggest that the cytokine-stimulated rise in p24 levels results from the expression of nascent 9-kb transcripts.

Characterization of the viral 2-kb message. Given that the 2-kb transcript was by far the most abundant transcript seen in viral persistence and with cytokine stimulation, we characterized the subpopulations of the multiply spliced transcripts by utilizing a previously described RT-PCR method (42). This method uses a set of primers in exon 1 (primer *Bss*) and exon 7 (primer *Bam*A) to amplify all of the multiply spliced transcripts simultaneously because these exons are present in all HIV-1 viral transcripts. Because the same primer pair and PCR mixture are used to identify all of the multiply spliced transcripts, the messages can be qualitatively compared when a probe is used to detect all of the regulatory transcripts. Given the position of the primers, the expected sizes of the amplification products from multiply spliced transcripts would be between 190 and 600 bp, with the Tat-coding transcripts producing the largest of the PCR products, Nef transcripts producing the smallest products, and Rev transcripts producing intermediate-sized products. The extension step of the cycling parameter was kept sufficiently short to prevent amplification of the unspliced or singly spliced transcripts. cDNA was synthesized by RT and the antisense primer *Bam*A, followed by PCR amplification with the addition of sense primer *Bss*. Amplification of the viral transcripts 2 days posttransfection gave a complex pattern of bands when the PCR products were run on a 1.5% agarose gel, transferred to a nylon membrane, and hybridized with an 8-kb *Ava*I fragment of pNL4-3. This fragment spans all of the exons of HIV-1 and would be expected to hybridize to all multiply spliced messages. As seen in Fig. 3, amplification of RNA 2 days posttransfection consistently gave a pattern of three sets of doublet bands ranging in size from 200 bp to almost 600 bp. In the first lane, 10 μl of the PCR mixture was loaded, while in the second lane 20 μl was loaded.

To identify the genomic regions present in the amplified cDNAs, the membrane was sequentially hybridized to a series of probes located in exons 2, 3, 4, 4a/b, and 5. Probe 4 *tat* hybridizes to the 5′ region of exon 4 upstream of the *tat* AUG. As seen in Fig. 4, probe 4 *tat* hybridized to the three uppermost cDNA bands, indicating that there are at least three different-

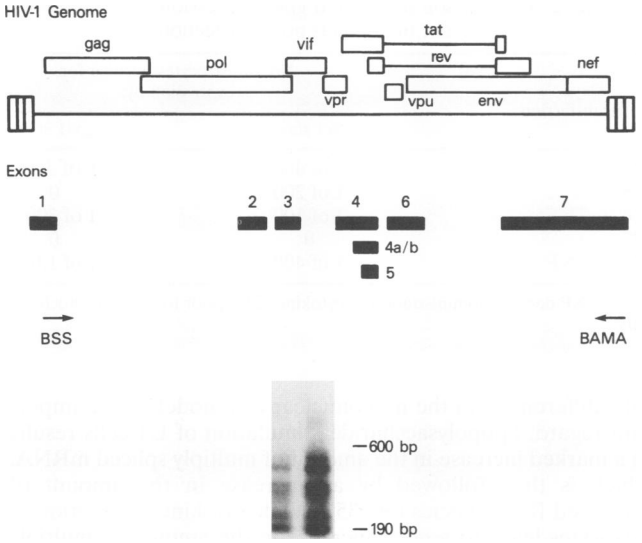

FIG. 3. RT-PCR amplification of the viral 2-kb messages. The top of the figure illustrates the open reading frames and exons of the HIV-1 genome. Exons are numbered according to the numbering of Meusing et al. (30) and Schwartz et al. (42). *Bss* and *Bam*A are previously described primers (42) in exons 1 and 7, respectively, used in the RT-PCR amplification step. The bottom of the figure shows the results of RT-PCR amplification and cDNA Southern hybridization of RNA extracted from astrocytes 2 days posttransfection with pNL4-3. In the first lane, 10 μl of the PCR mixture was loaded, while in the second lane 20 μl was loaded.

sized transcripts with the Tat-coding exon in these astrocytes. The uppermost of these three transcripts also hybridized to a probe for exon 2, identifying this band as a triple-spliced Tat transcript which contains exon 2 in addition to exons 1, 4, and 7. Probe 4a/b *tat/rev* hybridizes to a region of exon 4a/b spanning the *rev* AUG. Exon 4a/b is nested within exon 4 and will therefore hybridize to the Tat- and Rev-encoding transcripts as well. As seen in Fig. 4, probe 4a/b *tat/rev* hybridized to five transcripts, two more than the 4 *tat* probe. The two smallest bands correspond to Rev-specific transcripts. Of the two Rev-specific transcripts, the larger one also hybridized to the probe for exon 3, identifying it as a triple-spliced Rev transcript with exon 3 in addition to exons 1, 4a/b, and 7. Probe 5 *tat/rev/nef* hybridizes to the 5′ region of exon 5, an exon nested within exons 4 and 4a/b, which is present in all Tat-, Rev-, and Nef-encoding transcripts. This probe hybridized to all six transcripts, demonstrating that the smallest transcript seen is Nef specific.

Hybridization with the probes in exons 2 and 3 showed that these small noncoding exons were also present in a number of transcripts which did not hybridize to the Tat-, Rev-, or Nef-specific probes.

Temporal characteristics of Tat-, Rev-, and Nef-specific transcripts in astrocytes. We next analyzed the temporal characteristics of the regulatory transcripts identified by the RT-PCR methodology. RNA was extracted at different time points posttransfection, reverse transcribed, and PCR amplified as described above. Following Southern transfer to a nylon filter, the PCR products were hybridized with oligonucleotide probe 5 *tat/rev/nef* to determine which of the regulatory transcripts were present. As seen in Fig. 5, by day 15 posttransfection, the most prominent regulatory transcripts were those which coded for Nef and Rev. However, the addition of either TNF-α or IL-1β on day 15 posttransfection resulted in the induction of Nef-, Rev-, and Tat-specific transcripts by day 16. By day 27 posttransfection, no transcripts were detectable, either by Northern hybridization or RT-PCR, but again the addition of cytokines resulted in the induction of transcripts for all three regulatory elements. In all cases, the Nef-specific transcript was the strongest band present.

Supernatant taken from the astrocyte cultures at day 17 posttransfection (treated with TNF-α on day 15), which had a p24 level of 105 pg/ml and presumably viable NL4-3, was used to infect A3.01 cells, a $CD4^+$ T-cell line (19). Fifteen days after the initial infection, the A3.01 cells produced 2 ng of p24 per ml/day, confirming the presence of viable NL4-3 in the astrocyte supernatant. Cytoplasmic RNA was extracted from 1 million of the A3.01 cells and reverse transcribed and amplified with primers *Bss* and *Bam*A as described above. The resulting banding pattern by Southern hybridization with the *Ava*I fragment of pNL4-3, as seen in Fig. 5, is more complex than that seen in astrocytes.

Immunohistochemistry for Nef protein in persistently infected astrocytes. Given that the Nef- and Rev-specific transcripts were the most abundant transcripts at most time points posttransfection and given the prior observation that *rev* and *nef* gene transcripts can code for Nef protein (42), we examined astrocytes at different time points for expression of Nef protein as well as for expression of the structural protein gp41. As seen in Table 2, Nef was detectable by immunohistochemistry of astrocytes through at least day 15 posttransfection, while gp41 expression was absent after 15 days. Cytokine administration at day 15 roughly doubled the number of astrocytes which expressed Nef 24 h later. By 27 days posttransfection, neither gp41 nor Nef expression was detectable, but again, administration of cytokines increased Nef expression and, to a lesser degree, gp41 expression within 24 h.

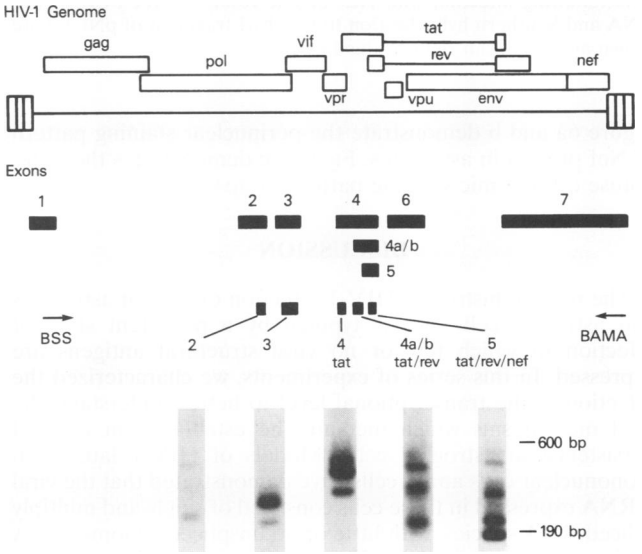

FIG. 4. Sequential Southern hybridization of RT-PCR-amplified 2-kb messages with oligonucleotide probes to different exons. RT-PCR amplification and Southern transfer were performed with RNA extracted from astrocytes 2 days posttransfection with pNL4-3. The filter was then sequentially hybridized to a series of oligonucleotide probes nested within exons 2 through 5. Beneath the exons of HIV-1 are shown the relative positions of the oligonucleotide probes used to identify the presence of the exons. The precise positions of the oligonucleotides are given in the text.

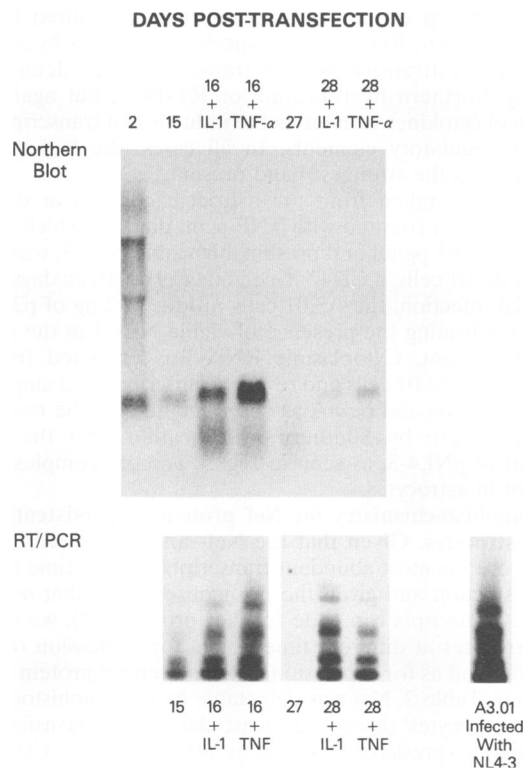

FIG. 5. Temporal characteristics of Tat-, Rev-, and Nef-specific transcripts in astrocytes. RNA previously extracted at different time points for use in Northern hybridization (see Fig. 1 and the top of this figure) was amplified with primers *Bss* and *Bam*A in an RT-PCR mixture and, following Southern transfer, was hybridized to oligonucleotide probe 5 *tat/rev/nef*, which is present in all Tat-, Rev-, and Nef-encoding transcripts. RNA was also extracted from A3.01 cells 15 days following infection with NL4-3. The results of RT-PCR of this RNA and Southern hybridization to the *Ava*I fragment of pNL4-3 are shown at the bottom right of this figure.

Figure 6a and b demonstrate the perinuclear staining pattern of Nef protein in astrocytes. Figure 6c demonstrates the more diffuse cytoplasmic staining pattern of gp41.

DISCUSSION

The natural history of HIV-1 infection of human astrocytes and astrocyte cell lines is typified by a persistent state of infection in which few or no viral structural antigens are expressed. In this series of experiments, we characterized the infection at the transcriptional level to better understand the viral mechanisms which mediate the establishment of viral persistence in astroglial cells. Models of HIV-1 latency in mononuclear cells and T cells have demonstrated that the viral mRNA expressed in these cells consisted of singly and multiply spliced RNA species, with little or no unspliced genomic RNA during chronic infection (30, 35). In primary human fetal astrocytes, a similar phenomenon is seen in which the predominant viral transcript during the establishment of persistence is multiply spliced. However, the astrocyte model is fundamentally different from the mononuclear cell model in one important regard; lipopolysaccharide stimulation of U1 cells results in a marked increase in the amount of multiply spliced mRNA, which is then followed by an increase in the amount of unspliced RNA species (30, 35). While cytokine stimulation of astrocytes leads to a clear increase in the amount of multiply spliced mRNA, no detectable increase in the amount of unspliced RNA is seen. This suggests that there is a critical difference in the physiology of astrocytes which prevents the accumulation of the unspliced HIV-1 viral transcript. This is of particular interest given the recent observation by Constantoulakis et al. (13) that there are interferon-inducible proteins in human cell types which bind to the responsive element, inhibiting function and resulting in an accumulation of the multiply spliced viral transcript. This would suggest that human fetal astrocytes have a similar factor or mechanism which may work at the level of the responsive element to give the mRNA patterns seen in Fig. 2. Work is being initiated in our laboratory to investigate this possibility.

TABLE 2. Comparison of Nef and gp41 expression in astrocytes at different time points posttransfection

Days posttransfection	No. of astrocytes positive for expression by:	
	Nef stain	gp41 stain
2	1 of 400	1 of 100
15	1 of 200	0
16 + TNF[a]	1 of 100	1 of 300
27	0	0
28 + TNF	1 of 400	1 of 1,000

[a] + TNF denotes administration of cytokines 24 h prior to immunocytochemistry.

The subpopulations of the 2-kb message are strikingly similar in both mononuclear cells and astrocytes in which HIV-1 has established a state of persistence. In H9 cells and peripheral blood monocyte-macrophages infected with HIV-1, the predominant multiply spliced transcript was the one which coded for Nef (23, 40). The Tat-specific mRNAs were the least abundant, while the Rev transcripts were intermediate in number. In the astrocyte model outlined, at times of persistence when the multiply spliced messages were the majority of the viral transcripts, the RT-PCR methodology found that the Nef- and Rev-encoding transcripts were the most abundant, with a predominance of the Nef-specific message, again similar to the mononuclear and lymphocytic cells (23, 40). Interestingly, Schwartz et al. (42) found that the transcripts for Rev and Nef both have open reading frames for Nef. Given the abundance of these transcripts and their increase during cytokine stimulation of astrocytes, the ability to detect Nef protein immunohistochemically is not surprising. The perinuclear location of Nef is consistent with findings from a persistently infected glioma cell line (24).

Could Nef, in addition to cellular factors, play a role in the establishment of a latent or persistent state of viral infection? This point remains controversial. In mononuclear cells, Nef was initially thought to be a negative regulator of viral expression at the level of the long terminal repeat. Similarly, in one astrocytoma model of HIV-1 infection, Nef also demonstrated a prominent suppression of the HIV long terminal repeat at

FIG. 6. Immunohistochemical identification of Nef protein and gp41 in astrocytes. Fig. 6a and b demonstrate the perinuclear localization of Nef protein in astrocytes. This is in contrast to gp41 expression, which is more diffusely cytoplasmic as seen in panel c.

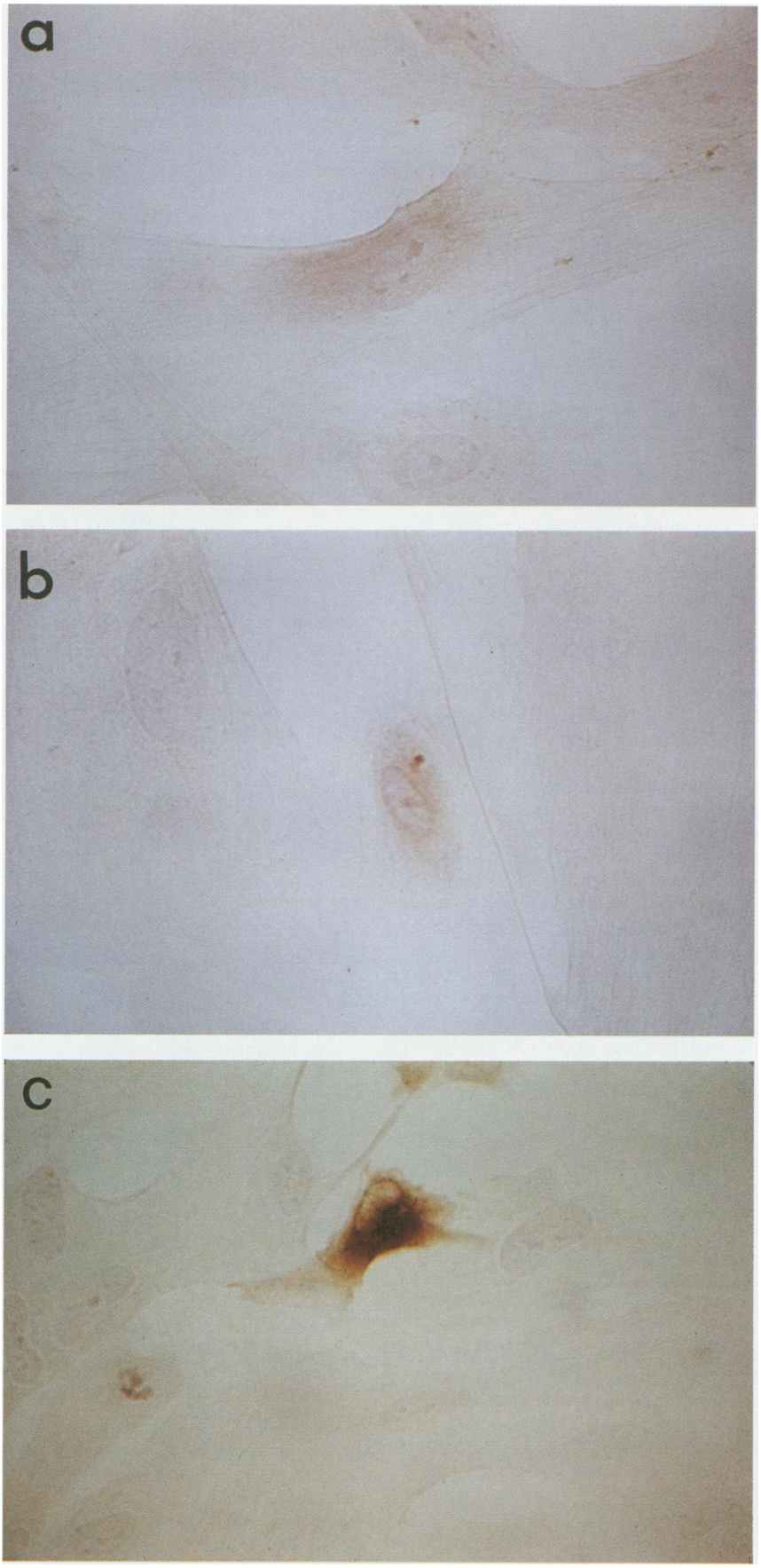
a
b
c

the level of the negative regulatory element (8). However, other investigators have observed no effect of Nef protein on either gene expression or viral replication in mononuclear and glial cell models (2, 22). Other functions attributed to the *nef* gene product which support its role in the establishment of viral persistence include (i) the ability to reduce cell surface expression of gp120 and CD4, presumably preventing the cytopathic effect of cell fusion (41), and (ii) inhibition of NF-κB induction, attenuating transcriptional upregulation at the level of the long terminal repeat (33). Interestingly, in the astrocyte model, we found an attenuation of expression of p24 and gp41 as well as that of the RNA transcripts over time. This probably does not reflect cell death, since the number of Nef-expressing cells remained relatively constant over time. Instead, one could postulate that Nef expression downregulated the long terminal repeat as well as blocked expression of structural proteins in these cells. Whatever its role, the fact that the Nef open reading frame is conserved in all primate lentiviruses and in pathological tissue (6) suggests that this protein plays a critical, and as yet undetermined, role in the viral life cycle.

The abundance of the multiply spliced transcripts found in astrocytes in vitro and their ability to code for Nef has significance for the detection of HIV-1-infected astrocytes in vivo. Studies to identify infected cells of the CNS in vivo generally use methods that target the viral structural proteins or genes coding for structural proteins. However, if the natural history of HIV-1 infection of astrocytes in vivo is also one of viral persistence in which the viral transcripts are restricted to the multiply spliced species, then detection methodology would have to be modified to reflect this. Specifically, immunohistochemical detection of infected astrocytes would have to target either Nef or Rev protein, since the structural and core proteins would be almost nonexistent, given the lack of the unspliced and singly spliced message in these cells. In situ detection of infected astrocytes would also have to use a nucleic acid probe which targets the exons present in the multiply spliced transcripts, since these are the most abundant viral nucleic acids. Probes which target exons or sequences outside these transcripts will probably fail to hybridize to infected astrocytes, again because the nonspliced or singly spliced viral transcripts are so few in number. Furthermore, the sensitivity of the probe would need to be maximized, given the restricted nature of the infection. Both our laboratory and that of Blumberg et al. (7) have taken this approach to identify infected astrocytes in vivo. Using a ^{32}P-labeled probe which contains the exons found in the HIV-1 multiply spliced transcripts and antibody to Nef protein, we were able to detect a small number of astrocytes which harbored HIV-1 nucleic acids in the subcortical white matter of 4 of 12 pediatric patients with AIDS encephalopathy (48). Blumberg et al., using monospecific *nef* probes and an antibody to Nef protein, also found evidence for HIV-1-infected astrocytes in postmortem CNS tissue from pediatric AIDS patients (7). With the advent of more sensitive detection techniques, such as in situ PCR (3, 16), the extent of glial infection may be further clarified.

The role infected astrocytes play in the pathogenesis of AIDS-associated dementia is unknown. While Nef protein has demonstrated functional similarities to scorpion peptides in its ability to interact with K^+ channels of chicken dorsal root ganglia (55), it is unclear whether infection disrupts the normal physiologic functions of astrocytes. Given the cytokine activation seen in vivo in the CNS of patients with AIDS encephalopathy (50), astrocytes could act as low-level producers of virion when exposed to these monokines, infecting surrounding tissue and infiltrating mononuclear cells. In addition to infecting the parenchymal elements, virions produced by astroglial elements may be directly toxic to the neuronal constituents. The uninfected, reactive astrocyte may also contribute to the neuropathology of HIV by releasing TNF-α when exposed to viral antigens (28). TNF-α is toxic to oligodendroglial cells (39, 43) and could contribute to the myelin pallor seen at autopsy. Reactive astrocytes in patients with AIDS dementia also produce transforming growth factor β, which may act as a chemoattractant for mononuclear cells into the CNS, further aggravating the encephalitis caused by HIV (52).

Finally, it appears that the natural history of HIV-1 infection of adult human astrocytes in vivo and in vitro may be different than that of astrocytes of the developing nervous system. One in vitro attempt to infect adult human astrocytes was unsuccessful (45), while in vivo detection of infected adult astrocytes has been inconsistent (38, 46, 53, 56). The immaturity of the glial elements in utero, as well as the immaturity of the pediatric immune system in the perinatal period, could in theory make the developing CNS more susceptible to viral invasion (26, 27) than the mature nervous system.

ACKNOWLEDGMENTS

We thank Renee Traub and Blanche Curfman for technical and editorial assistance. The anti-Nef monoclonal antibody from James Hoxie was obtained through the AIDS Research and Reference Reagent Program, Division of AIDS, NIAID.

REFERENCES

1. **Adachi, A., H. E. Gendelman, S. Koenig, T. Folks, R. Willey, A. Rabson, and M. A. Martin.** 1986. Production of acquired immunodeficiency syndrome-associated retrovirus in human and nonhuman cells transfected with an infectious molecular clone. J. Virol. **59**:284–291.
2. **Bachelerie, F., J. Alcami, U. Hazan, N. Israël, B. Goud, F. Arenzana-Seisdedos, and J.-L. Virelizer.** 1990. Constitutive expression of human immunodeficiency virus (HIV) *nef* protein in human astrocytes does not influence basal or induced HIV long terminal repeat activity. J. Virol. **64**:3059–3062.
3. **Bagasra, O., S. P. Hauptman, H. W. Lischner, M. Sachs, and R. J. Pomerantz.** 1992. Detection of human immunodeficiency virus type 1 provirus in mononuclear cells by in situ polymerase chain reaction. N. Engl. J. Med. **326**:1385–1391.
4. **Belman, A. L., M. H. Ultmann, D. Horoupian, B. Novick, A. J. Spiro, A. Rubinstein, D. Kurtzberg, and B. Cone-Wesson.** 1985. Neurological complications in infants and children with acquired immune deficiency syndrome. Ann. Neurol. **18**:560–566.
5. **Bernton, E., H. Bryant, M. Decoster, J. M. Ornestein, J. L. Ribas, M. S. Meltzer, and H. E. Gendelman.** 1992. No direct neurotoxicity by HIV-1 virions or culture fluids from HIV-1 infected T-cells or monocytes. AIDS Res. Hum. Retroviruses **8**:495–501.
6. **Blumberg, B. M., L. G. Epstein, Y. Saito, D. Chen, L. R. Sharer, and R. Anand.** 1992. Human immunodeficiency virus type 1 *nef* quasispecies in pathological tissue. J. Virol. **66**:5256–5264.
7. **Blumberg, B. M., L. R. Sharer, Y. Saito, J. Michaels, T. A. Cvetkovich, M. Louder, K. Golding, and L. Epstein.** Overexpression of nef is a marker for restricted HIV-1 infection of astrocytes in human CNS tissue. Neurology, in press.
8. **Brack-Werner, R., A. Kleinschmidt, A. Ludvigsen, W. Mellert, M. Neumann, R. Herrmann, M. C. L. Khim, A. Burny, N. Muller-Lantzsch, D. Stavrou, and V. Erfle.** 1992. Infection of human brain cells by HIV-1: restricted virus production in chronically infected human glial cell lines. AIDS **6**:273–285.
9. **Brenneman, D. E., G. L. Westbrook, S. P. Fitzgerald, D. L. Ennist, K. L. Elkins, M. R. Ruff, and C. B. Pert.** 1988. Neuronal cell killing by the envelope protein of HIV and its prevention by vasoactive intestinal peptide. Nature (London) **335**:639–642.
10. **Cheng-Mayer, C., J. T. Rutka, M. L. Rosenblum, T. McHugh, D. P. Stites, and J. Levy.** 1987. Human immunodeficiency virus can productively infect cultured human glial cells. Proc. Natl. Acad.

Sci. USA **84:**3526–3529.
11. **Chiodi, F., S. Fuerstenberg, M. Gidlund, B. Åsjö, and E. M. Fenyö.** 1987. Infection of brain-derived cells with the human immunodeficiency virus. J. Virol. **61:**1244–1247.
12. **Christofonis, G., L. Papadaki, Q. Sattentau, R. Ferns, and R. Tedder.** 1987. HIV replicates in cultured human brain cells. AIDS **1:**229–234.
13. **Constantoulakis, P., M. Campbell, B. K. Felber, G. Nasioulas, E. Afonina, and G. M. Pavlakis.** 1993. Inhibition of Rev-mediated HIV-1 expression by an RNA binding protein encoded by the interferon-inducible 9-27 gene. Science **259:**1314–1317.
14. **Dewhurst, S., K. Sakai, J. Bresser, M. Stevenson, M. J. Evinger-Hodges, and D. J. Volsky.** 1987. Persistent productive infection of human glial cells by human immunodeficiency virus (HIV) and by infectious molecular clones of HIV. J. Virol. **61:**3774–3782.
15. **Dreyer, E. B., P. K. Kaiser, J. T. Offerman, and S. A. Lipton.** 1990. HIV-1 coat protein neurotoxicity prevented by calcium channel antagonists. Science **248:**364–367.
16. **Embretson, J., M. Zupancic, J. Beneke, M. Till, S. Wolinsky, J. L. Ribas, A. Burke, and A. T. Haase.** 1993. Analysis of human immunodeficiency virus-infected tissues by amplification and in situ hybridization reveals latent and permissive infections at single-cell resolution. Proc. Natl. Acad. Sci. USA **90:**357–361.
17. **Epstein, L. G., L. R. Sharer, E.-S. Cho, M. Myenhofer, B. Navia, and R. Price.** 1984. HTLV-III/LAV-like retrovirus particles in the brains of patients with AIDS encephalopathy. AIDS Res. Hum. Retroviruses **1:**447–454.
18. **Epstein, L. G., L. R. Sharer, V. V. Joshi, M. M. Fojas, M. R. Koenigsberger, and J. M. Oleske.** 1985. Progressive encephalopathy in children with acquired immune deficiency syndrome. Ann. Neurol. **17:**488–496.
19. **Folks, T., S. Benn, A. Rabson, T. Theodore, M. Hoggan, M. Martin, M. Lightfoote, and K. Sell.** 1985. Characterization of a continuous T cell line susceptible to the cytopathic effects of the acquired immunodeficiency syndrome (AIDS)-associated retrovirus. Proc. Natl. Acad. Sci. USA **82:**4539–4543.
20. **Genis, P., M. Jett, E. W. Bernton, T. Boyle, H. A. Gelbard, K. Dzenko, R. W. Keane, L. Resnick, Y. Mizrachi, D. J. Volsky, L. G. Epstein, and H. E. Gendelman.** 1992. Cytokines and arachidonic acid metabolites produced during HIV-infected macrophage-astroglial interactions: implications for the neuropathogenesis of HIV disease. J. Exp. Med. **176:**1703–1718.
21. **Giulian, D., K. Vaca, and C. A. Noonan.** 1990. Secretion of neurotoxins by mononuclear phagocytes infected with HIV-1. Science **250:**1593–1596.
22. **Hammes, S. R., E. P. Dixon, M. H. Malim, B. R. Cullen, and W. C. Greene.** 1989. Nef protein of human immunodeficiency virus type 1: evidence against its role as a transcriptional inhibitor. Proc. Natl. Acad. Sci. USA **86:**9549–9553.
23. **Klotman, M. E., K. Sunyoung, A. Buchbinder, A. DeRossi, D. Baltimore, and F. Wong-Staal.** 1991. Kinetics of expression of multiply spliced RNA in early human immunodeficiency virus type 1 infection of lymphocytes and monocytes. Proc. Natl. Acad. Sci. USA **88:**5011–5015.
24. **Kohleisen, B., M. Neumann, R. Herrman, R. Brack-Werner, K. Krohn, V. Ovod, A. Ranki, and V. Erfle.** 1992. Cellular localization of Nef expressed in persistently HIV-1-infected low-producer astrocytes. AIDS **6:**1427–1436.
25. **Lipton, S. A., N. J. Sucher, P. K. Kaiser, and E. B. Dreyer.** 1991. Synergistic effects of HIV coat protein and NMDA receptor-mediated neurotoxicity. Neuron **7:**111–118.
26. **Lyman, W. D., Y. Kress, K. Kure, W. Rashbaum, A. Rubinstein, and R. Soeiro.** 1990. Detection of HIV in fetal central nervous system tissue. AIDS **4:**917–920.
27. **Mano, H., and J.-C. Chermann.** 1991. Fetal human immunodeficiency virus type 1 infection of different organs in the second trimester. AIDS Res. Hum. Retroviruses **7:**83–88.
28. **Merrill, J. E., Y. Koyanagi, J. Zack, L. Thomas, F. Martin, and I. S. Y. Chen.** 1992. Induction of interleukin-1 and tumor necrosis factor alpha in brain cultures by human immunodeficiency virus type 1. J. Virol. **66:**2217–2225.
29. **Michael, N. L., P. Morrow, J. Mosca, M. Vahey, D. S. Burke, and R. R. Redfield.** 1991. Induction of human immunodeficiency virus type 1 expression in chronically infected cells is associated primarily with a shift in RNA splicing patterns. J. Virol. **65:**1291–1303.
30. **Muesing, M. A., D. H. Smith, C. D. Cabradilla, C. V. Benton, L. A. Lasky, and D. J. Capon.** 1985. Nucleic acid structure and expression of the human AIDS/lymphadenopathy retrovirus. Nature (London) **313:**450–458.
31. **Navia, B. A., E.-S. Cho, C. K. Petito, and R. W. Price.** 1986. The AIDS dementia complex. II. Neuropathology. Ann. Neurol. **19:** 525–535.
32. **Navia, B. A., B. D. Jordan, and R. W. Price.** 1986. The AIDS dementia complex. I. Clinical features. Ann. Neurol. **19:**517–524.
33. **Niederman, T. M. J., J. V. Garcia, W. R. Hastings, S. Luria, and L. Ratner.** 1992. Human immunodeficiency virus type 1 Nef protein inhibits NF-κB induction in human T cells. J. Virol. **66:**6213–6219.
34. **Novella, A. C., P. H. Wise, A. Willoughby, and P. A. Pizzo.** 1989. Final report of the United States Department of Health and Human Services Secretary's work group on pediatric human immunodeficiency virus infection and disease: content and implications. Pediatrics **84:**547–555.
35. **Pomerantz, R. J., T. Didier, M. B. Feinberg, and D. Baltimore.** 1990. Cells nonproductively infected with HIV-1 exhibit an aberrant pattern of viral RNA expression: a molecular model for latency. Cell **61:**1271–1276.
36. **Price, R. W., B. Brew, J. Sidtis, M. Rosenblum, A. C. Scheck, and P. Cleary.** 1988. The brain in AIDS: central nervous system infection and AIDS dementia complex. Science **239:**586–593.
37. **Pulliam, L., B. G. Herndier, N. M. Tang, and M. S. McGrath.** 1991. Human immunodeficiency virus-infected macrophages produce soluble factors that cause histological and neurochemical alterations in cultured human brains. J. Clin. Invest. **87:**503–512.
38. **Rhodes, R. H., and J. M. Ward.** 1991. AIDS meningoencephalitis. Pathogenesis and changing neuropathologic findings. Pathol. Annu. **26:**247–276.
39. **Robbins, D. S., Y. Shirazi, B.-E. Drysdale, A. Lieberman, H. S. Shin, and M. L. Shin.** 1987. Production of cytotoxic factors for oligodendrocytes by stimulated astrocytes. J. Immunol. **139:**2593–2597.
40. **Robert-Guroff, M., M. Popovic, S. Gartner, P. Markham, R. C. Gallo, and M. S. Reitz.** 1990. Structure and expression of *tat*-, *rev*-, and *nef*-specific transcripts of human immunodeficiency virus type 1 in infected lymphocytes and macrophages. J. Virol. **64:**3391–3398.
41. **Schwartz, O., Y. Rivière, J.-M. Heard, and O. Danos.** 1993. Reduced cell surface expression of processed human immunodeficiency virus type 1 envelope glycoprotein in the presence of Nef. J. Virol. **67:**3274–3280.
42. **Schwartz, S., B. K. Felber, D. M. Benko, E.-M. Fenyö, and G. N. Pavlakis.** 1990. Cloning and functional analysis of multiply spliced mRNA species of human immunodeficiency virus type 1. J. Virol. **64:**2519–2529.
43. **Selmaj, K. W., and C. S. Raine.** 1988. Tumor necrosis factor mediates myelin and oligodendrocyte damage in vitro. Ann. Neurol. **23:**339–346.
44. **Sharer, L. R., L. G. Epstein, E.-S. Cho, V. V. Joshi, M. F. Meyenhofer, L. F. Rankin, and C. K. Petito.** 1986. Pathologic features of AIDS encephalopathy in children: evidence for LAV/HTLV III infection of brain. Hum. Pathol. **17:**271–284.
45. **Sharpless, N., D. Gilbert, B. Vandercam, J. M. Zhou, E. Verdin, G. Ronnett, E. Friedman, and M. Dubois-Dalcq.** 1992. The restricted nature of HIV-1 tropism for cultured neural cells. Virology **191:**813–825.
46. **Stoler, M. H., T. A. Eskin, S. Benn, R. C. Angerer, and L. M. Angerer.** 1986. Human T-cell lympho-tropic virus type III infection of the central nervous system—a preliminary in situ analysis. JAMA **256:**2360–2364.
47. **Swingler, S., A. Easton, and A. Morris.** 1992. Cytokine augmentation of HIV-1 LTR driven gene expression in neural cells. AIDS Res. Hum. Retroviruses **8:**487–493.
48. **Tornatore, C. S., R. Chandra, J. Berger, and E. O. Major.** HIV-1 infection of subcortical astrocytes in the pediatric central nervous system. Neurology, in press.
49. **Tornatore, C., A. Nath, K. Amemiya, and E. O. Major.** 1991.

Persistent human immunodeficiency virus type 1 infection in human fetal glial cells reactivated by T-cell factor(s) or by the cytokines tumor necrosis factor alpha and interleukin-1 beta. J. Virol. **65:**6094–6100.

50. **Tyor, W. R., J. D. Glass, J. W. Griffin, and P. S. Becker.** 1992. Cytokine expression in the brain during the acquired immunodeficiency syndrome. Ann. Neurol. **31:**349–360.
51. **Vitkovic, L., G. P. Wood, E. O. Major, and A. S. Fauci.** 1991. Human astrocytes stimulate HIV-1 expression in a chronically infected promonocyte clone via interleukin-6. AIDS Res. Hum. Retroviruses **7:**723–727.
52. **Wahl, S. M., J. B. Allen, N. McCartney-Francis, M. C. Morganti-Kossmann, T. Kossman, L. Ellingsworth, U. E. H. Mai, S. E. Mergenhagen, and J. M. Orenstein.** 1991. Macrophage- and astrocyte-derived transforming growth factor beta as a mediator of central nervous system dysfunction in acquired immune deficiency syndrome. J. Exp. Med. **173:**981–991.
53. **Ward, J. M., T. J. O'Leary, G. B. Baskin, R. Benveniste, C. A. Harris, P. L. Nara, and R. H. Rhodes.** 1987. Immunohistochemical localization of human and simian immunodeficiency viral antigens in fixed tissue sections. Am. J. Pathol. **127:**199–205.
54. **WenQin, X., and L. I. Rothblum.** 1991. Rapid, small-scale RNA isolation from tissue culture cells. BioTechniques **11:**324–327.
55. **Werner, T., S. Ferroni, T. Saermark, R. Brack-Werner, R. B. Banati, R. Mager, L. Steinaa, G. W. Kreutzberg, and V. Erfle.** 1991. HIV-1 Nef protein exhibits structural and functional similarity to scorpion peptides interacting with K^+ channels. AIDS **5:**1301–1308.
56. **Wiley, C. A., R. D. Schrier, J. A. Nelson, P. W. Lampert, and M. B. A. Oldstone.** 1986. Cellular localization of human immunodeficiency virus infection within the brains of acquired immune deficiency syndrome patients. Proc. Natl. Acad. Sci. USA **83:**7089–7093.